

Research on Microstructure Evolution of Hot Deformation of Ti40 Alloy

Qiaoyu Pan ¹, Wei Meng², Xinping Yu ¹, Guangyong Pan ¹, Qinghua Huang ¹,
Yongjie Qi ¹

¹Zhejiang Guangsha Vocational and Technical University of Construction, Dongyang, 322100, China

²Hangzhou Vocational and Technical college, Hangzhou 31000, China

Abstract

Hot compression test and microstructure simulation were carried out for Ti40 alloy. The results show that under certain deformation conditions, with the increase of strain, the volume fraction of dynamic recrystallization increases continuously, and the average grain size is refined continuously, and the relative error is less than 10%. The simulated microstructure of the alloy under different deformation conditions was observed. When the deformation temperature is constant, the dynamic recrystallization can be promoted by reducing the strain rate, and the average grain size can be refined. When the strain rate is constant, increasing temperature can not only promote the occurrence of dynamic recrystallization, but also promote the growth of recrystallized grains.

Keywords

Ti40 alloy; microstructure; dynamic recrystallization.

1. Introduction

Existing studies have found that Ti40 alloy has poor workability and cracks on the surface or inside the structure, making it difficult to control the hot working process and limiting the application of this alloy [1]. Therefore, it is of great significance to improve the ductility of the alloy to overcome the poor workability of the alloy during the hot working process. Aiming at Ti40 alloy, Zhang Xuemin et al. [2] studied the dynamic softening behavior of coarse-grained alloy during superplastic deformation, and showed that the fine recrystallized grains coordinated the deformation and can make it obtain better superplastic properties; Lai et al. [3] Studies have shown that the coarse grain structure and improper forging process of the alloy can easily cause cracks in the grain boundary under the condition of large deformation, but the reduction of the grain size can increase the grain boundary per unit area, thereby improving the deformability and reducing the deformation resistance; Zhu Yanchun et al. [4] showed that the higher the strain rate, the more serious the alloy cracking. In addition, the temperature increases, the critical cracking deformation increases, and the crack propagation speed slows down. The essence of the thermal deformation process is the influence of thermal deformation parameters on softening mechanisms such as dynamic recrystallization. It can be seen that searching for better deformation parameters to refine the structure grains through dynamic recrystallization plays an important role in improving the plastic properties of Ti40 alloy.

Metal material forming blanks are mostly processed by extrusion, forging, ring rolling and bar stock processing. Among them, ring rolling is a more effective blank forming method for the powerful spinning forming of Ti40 alloy combustion cylinders [5]. In view of this, this article conducts a cylindrical hot compression test for the ring-rolled Ti40 alloy, establishes the flow stress constitutive equation, dynamic recrystallization mathematical model, and combines the DEFORM-3D finite element software to simulate and analyze the effect of thermal deformation

parameters on dynamic recrystallization and other microstructures. The impact of changes is expected to provide a reference for the formulation of related thermal processing techniques.

2. Experimental materials and methods

The experimental material was a ring-rolled Ti40 alloy billet provided by a company. The material was processed into a cylindrical specimen of $\text{Ø}8 \text{ mm} \times 12 \text{ mm}$ by wire cutting, and the hot compression test was performed on the Gleeble-3800 thermal simulator. In order to prevent severe bulging during the thermal compression of the sample, tantalum and graphite sheets were placed on the upper and lower ends of the sample, and molybdenum disulfide lubricant was used. A platinum-platinum rhodium thermocouple was spot welded on the surface of the sample to record and control the deformation temperature. The thermal compression process first heats up to the corresponding temperature at a rate of 10°C/s , and heats it after holding for 3 minutes. The thermal compression temperature T : 950, 1000, 1050, 1100 $^\circ\text{C}$, strain rate $\dot{\varepsilon}$: 0.001, 0.01, 0.1, 1s^{-1} , The amount of strain ε (% compression) is 0.11 (10%), 0.22 (20%), 0.51 (40%), 0.92 (60%). Immediately after deformation, water-cooled, and finally observed the microstructure with a metallurgical microscope.

3. Experimental results and discussion

3.1. Flow stress curve

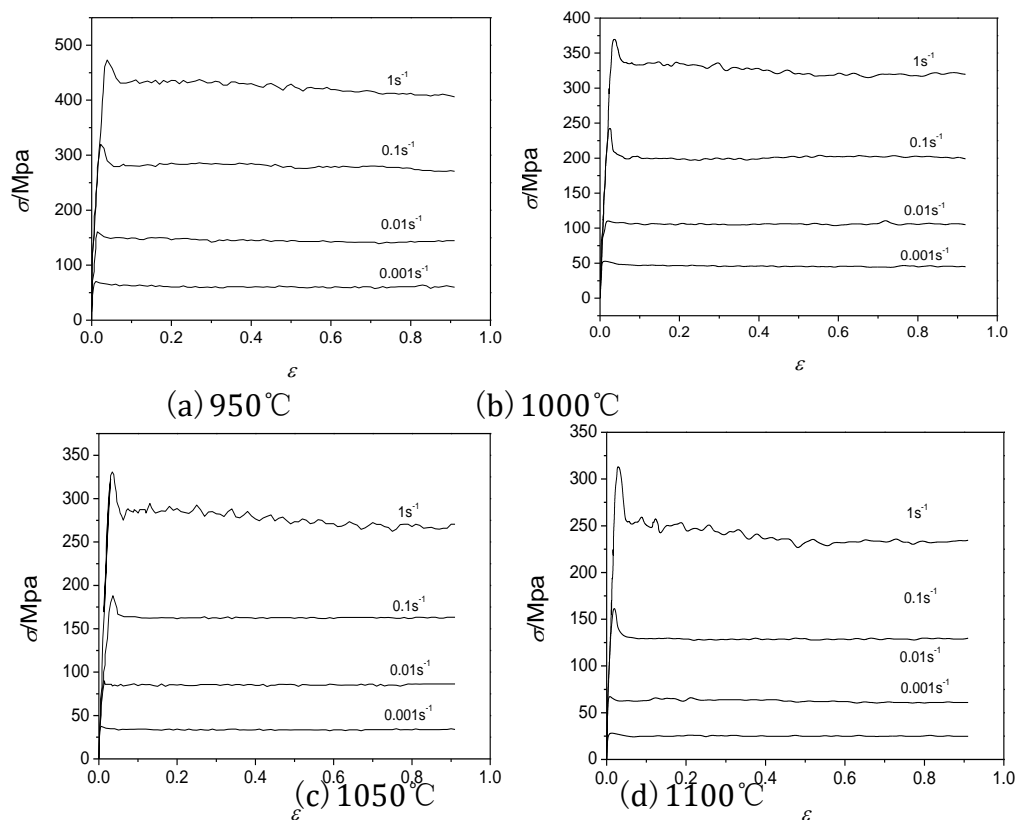


Fig.1 Stress-strain curves of Ti40 alloy under different deformation conditions

Figure 1 shows the flow stress curve of Ti40 alloy under different deformation conditions. When the temperature is constant, the flow stress increases with the increase of the strain rate, and when the strain rate is constant, the flow stress decreases with the increase of the temperature. In the initial small deformation range, the stress rapidly increases from zero to a

large value. This is due to the work hardening behavior caused by the proliferation of dislocations. Then the deformation increases, the stress decreases, and then tends to stabilize or decrease slowly. The curve as a whole shows a single peak shape of discontinuous dynamic recrystallization.

3.2. Flow stress constitutive equation

Under the condition of hot deformation of Ti40 alloy, the relationship between flow stress σ , strain rate $\dot{\varepsilon}$ and temperature T can be expressed by the Arrhenius relationship [6]:

$$\dot{\varepsilon} = A [\sinh(\alpha\sigma)]^n \exp[-Q/(RT)] \quad (1)$$

In the formula: A , n and α are all constants; Q is the thermal deformation activation energy, $\text{KJ}\cdot\text{mol}^{-1}$; R is the gas constant, $8.314\text{J}\cdot(\text{mol}\cdot\text{k})^{-1}$. Take the logarithm of equation (1), and based on the flow stress curve data, linearly regress the coefficients in the equation [6-7], and substitute them into the above equation, as shown below:

$$\dot{\varepsilon} = 2.0878334 \times 10^7 [\sinh(0.006429\sigma)]^{2.363575} \times \exp[-223.684 \times 10^3 / RT] \quad (2)$$

3.3. JMAK mathematical model of dynamic recrystallization

It can be seen that the dynamic recrystallization of the alloy during hot deformation is essentially the result of dislocation proliferation, but the movement of dislocations cannot be dynamically observed, but the change law of the flow stress curve during the hot deformation can more intuitively reflect the occurrence of dynamic recrystallization. To the end, when the dislocation density multiplies to a certain critical value, the strain corresponding to the curve at this time is the critical strain ε_c for dynamic recrystallization. Research by Sellars et al. believes that the critical strain ε_c and the peak strain ε_p are in a certain proportion [8], and Establish an empirical formula, namely $\varepsilon_c = (0.6 \sim 0.85) \varepsilon_p$. The peak strain can be directly observed from the curve and is related to strain rate, deformation temperature and initial grain size. It can be expressed by the JMAK mathematical model [9], as shown in equation (9):

$$\varepsilon_p = a_1 d_0^{n_1} \dot{\varepsilon}^{m_1} \exp(Q_1 / RT) \quad (3)$$

In the formula, a_1 , n_1 , m_1 and Q_1 are the fitting constants; $\dot{\varepsilon}$ is the strain rate; T thermal deformation temperature, K ; d_0 initial grain size, $200\mu\text{m}$; R gas constant, $8.314\text{J}\cdot\text{mol}^{-1}\cdot\text{k}^{-1}$.

During the hot deformation of the alloy, the volume fraction of dynamic recrystallization changes with the increase of strain and is reflected on the curve, showing a certain law, which can be expressed by equation (4) [9]:

$$X_{\text{dyn}} = 1 - \exp\left(-k_1 (\varepsilon - \varepsilon_c) / \varepsilon_{0.5}\right)^{k_2} \quad (4)$$

In the formula, k_1 and k_2 are fitting constants; X_{dyn} is the dynamic recrystallization volume fraction; $\varepsilon_{0.5}$ is the strain when 50% dynamic recrystallization occurs, which can be expressed by equation (5) [9]:

$$\varepsilon_{0.5} = a_2 d_0^{n_2} \dot{\varepsilon}^{m_2} \exp(Q_2 / RT) \quad (5)$$

In the formula, a_1 , n_1 , m_1 and Q_2 are fitting constants. Among them, the dynamic recrystallized grain size d_{dyn} can be expressed by equation (6) [9]:

$$d_{\text{dyn}} = a_3 d_0^{h_3} \varepsilon^{n_3} \dot{\varepsilon}^{m_3} \exp(Q_3 / RT) \quad (6)$$

In the formula, a_3 , h_3 , n_3 , m_3 , and Q_3 are fitting constants. The grains of the structure during the deformation process will include recrystallized grains and unrecrystallized grains, and the average grain size can be expressed by equation (7) [9]:

$$d_{\text{avg}} = d_{\text{dyn}} X_{\text{dyn}} + d_0 (1 - X_{\text{dyn}}) \quad (7)$$

In the formula, d_{avg} is the average grain size during thermal deformation.

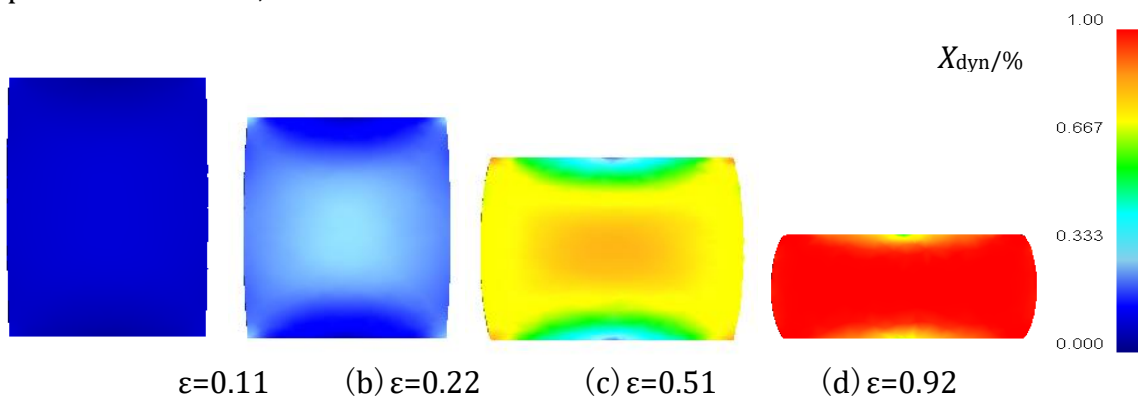
Based on statistics of the peak stress and metallographic grain size of Ti40 alloy at 950~1100°C and 0.001~1s⁻¹ deformation conditions, linear fitting is performed, and the relevant data of the above equation is shown in equation (8).

$$\begin{cases} \varepsilon_c = 0.83\varepsilon_p \\ \varepsilon_p = 0.00057d_o^{-0.267} \dot{\varepsilon}^{0.195} \exp(60726 / RT) \\ X_{dyn} = 1 - \exp\left(-0.693(\varepsilon - \varepsilon_c) / \varepsilon_{0.5}\right)^2 \\ \varepsilon_{0.5} = 0.00395d_o^{0.494} \dot{\varepsilon}^{0.252} \exp(40097 / RT) \\ d_{dyn} = 54284d_o^{0.291} \varepsilon^{0.429} \dot{\varepsilon}^{-0.38} \exp(-119961 / RT) \end{cases} \quad (8)$$

3.4. Simulation of organizational evolution

The flow stress constitutive model and the dynamic recrystallization JMAK mathematical model obtained from the foregoing calculations are implanted into the DEFORM-3D finite element software platform, and combined with the software cellular automata organization evolution module, the dynamic recrystallization microstructure is quantified and visualized Evolution simulation.

The alloy is subjected to thermal compression simulation at 1050°C and 0.001s⁻¹, and the dynamic recrystallization volume fraction X_{dyn} and the average grain size d_{avg} change cloud diagram, as shown in Figure 3 (a ~ h). It can be seen that when the strain reaches 0.11 (10%), dynamic recrystallization begins to occur in the large deformation area in the center of the sample, X_{dyn} is 6.26%, and d_{avg} is 189μm. As the strain increases, the dynamic recrystallization area of the sample gradually expands. When the variable is 0.51 (40%), the X_{dyn} in the center area of the sample is 85.2%, and the d_{avg} is 71.8μm. After the thermal compression is completed, except for the upper and lower contact deformation areas of the sample, the dynamic recrystallization occurs completely at other positions, and X_{dyn} reaches 100% , d_{avg} is 54.7μm. Combined with the metallographic observation of the metallographic structure in the large deformation zone of the sample, as shown in Figure 4 (a to d), when the strain reaches 0.22 (20%), a relatively small dynamic precipitation occurs at the grain boundary of the large β grains in the structure. Crystal grains, d_{avg} is 165.5μm, when the amount of strain reaches 0.51 (40%), the number of dynamic recrystallized grains increases, the volume fraction of dynamic recrystallization reaches over 85%, the average grain size d_{avg} is 75.3μm, and the strain reaches 0.92 When the d_{avg} is 58.62μm. The comparison shows that the quantified simulation results based on the dynamic recrystallization JMAK mathematical model are in good agreement with the experimental results, and the relative error is within 10%.



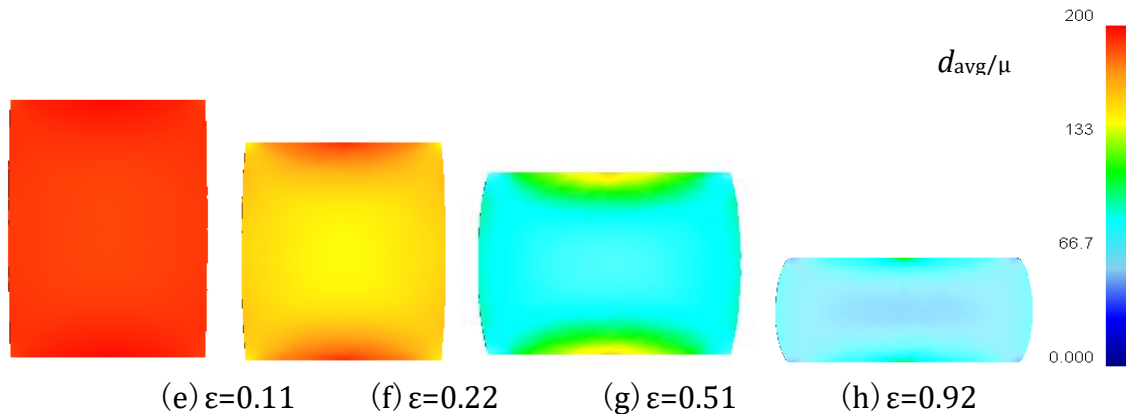


Fig. 3 The X_{dyn} and d_{avg} change cloud diagram of Ti40 alloy at 1050°C, 0.001s⁻¹ deformation conditions under different strain

4. Conclusion

(1) For the ring-rolled Ti40 alloy, conduct a hot compression test at 950~1100°C and 0.001~1s⁻¹ deformation on the Gleeble-3500 type hot compression tester. The equation of flow stress and the mathematical model of dynamic recrystallization are established by linear regression method based on the test data.

(2) Based on the mathematical model of dynamic recrystallization, quantitative and visualized microstructure evolution simulation on DEFORM-3D finite element software platform. It can be seen that at 1050°C and 0.001s⁻¹, as the strain increases, X_{dyn} continues to increase, and d_{avg} continues to refine. When the strain reaches 0.92, the d_{avg} is 58.62μm. Compared with the experimental data, the relative error is within 10%.

Acknowledgments

The work described in this paper was fully supported by Scientific Research Project of Zhejiang Education Department (Y202044336).

References

- [1] Yan-chun Zhu, Wei-dong Zeng, Yong-qing Zhao, et al. Effect of processing parameters on hot deformation behavior and microstructural evolution during hot compression of Ti40 titanium alloy[J]. Materials Science and Engineering A, 2012, 552: 384-391.
- [2] Zhang Xuemin, Zeng Weidong, Li Yue, et al. Dynamic softening behavior of coarse-grained Ti40 alloy during superplastic deformation[J]. Rare Metal Materials and Engineering, 2019, 48(10): 3202-3208.
- [3] Yun-jin Lai, She-wei Xin, Ping-xiang Zhang, et al. Recrystallization behavior of Ti40 burn-resistant titanium alloy during hot working process[J]. International Journal of Minerals Metallurgy and Materials, 2016, 23(05): 581-587.
- [4] Zhu Yanchun, Zeng Weidong, Peng Wenwen, et al. Cracking behavior of Ti40 alloy during hot compression deformation[J]. Rare Metal Materials and Engineering, 2013, 42(10): 2088-2092.
- [5] Zhang Cheng, Yang Haicheng, Han Dong, et al. Application and development of titanium alloy spinning technology in the domestic aerospace field. Solid Rocket Technology, 2013, 36(1): 127-132.
- [6] Wang Xin, Dong Hongbo, Zou Zhongbo, et al. Hot deformation microstructure evolution and dynamic recrystallization behavior of AerMet100 steel[J]. Special Casting & Nonferrous Alloys, 2016, 36(1): 121-125.
- [7] Ni Hongming, Dong Xianjuan, Xu Yong, et al. Hot deformation behavior and constitutive relationship of Ti-48Al-2Nb-2Cr alloy[J]. Special Casting and Nonferrous Alloys, 2020, 40(02): 228-232.

- [8] Sellars C M, Whiteman J A. Recrystallization and grain growth in hot rolling[J]. Metal Science, 1979, 13(3): 187-194.
- [9] Guo Hailong, Sun Zhichao, Yang He. Empirical model and application of extruded 7075 aluminum alloy recrystallization[J]. The Chinese Journal of Nonferrous Metals, 2013, 23(06): 1507-1515.